Original Article

A diagnostic test of three-dimensional magnetic resonance elastography imaging for preoperative prediction of microvascular invasion in patients with T1 stage clear cell renal carcinoma

Han-Mei Zhang[1], Da-Guang Wen[1], Jie Chen[1], Yun-Tian Chen[1], Meng Yin[2], Yi Wang[1], Yi Wei[1], Yi-Ge Bao[3], Ying-Hua Wu[4], Bin Song[1]

[1]Department of Radiology, Sichuan University West China Hospital, Chengdu, China; [2]Department of Radiology, Mayo Clinic, Rochester, MN, USA; [3]Department of Urology, Sichuan University West China Hospital, Chengdu, China; [4]Department of Radiology, The Clinical Medicine School, Chengdu University of Traditional Chinese Medicine, Chengdu, China

Contributions: (I) Conception and design: HM Zhang; (II) Administrative support: M Yin, B Song; (III) Provision of study materials or patients: DG Wen, J Chen, YH Wu; (IV) Collection and assembly of data: YG Bao, YT Chen; (V) Data analysis and interpretation: Y Wang, Y Wei; (VI) Manuscript writing: All authors; (VII) Final approval of manuscript: All authors.

Correspondence to: Bin Song, MD. Department of Radiology, Sichuan University West China Hospital, No. 37, Guo Xue Xiang, Chengdu 610041, China. Email: songlab_radiology@163.com.

Background: Detection of microvascular invasion (MVI) of kidney tumors is important for selecting the optimal therapeutic strategy. Currently, the prediction of MVI lacks an accurate imaging biomarker. This study evaluated the performance of three-dimensional (3D) magnetic resonance elastography (MRE) imaging in predicting microvascular invasion (MVI) of T1 stage clear cell renal carcinoma (ccRCC).

Methods: In this prospective study, we conducted pre-surgical imaging with a clinical 3.0 T magnetic resonance imaging (MRI) system. Firstly, 83 consecutive patients were enrolled in this study. A 3D MRE stiffness map was generated and transferred to a post-processing workstation. Contrast-enhanced computed tomography (CT) was conducted to calculate the tumor enhancement ratio. The presence of MVI was evaluated by histopathological analysis and graded according to the risk stratification based upon the number and distribution. The mean stiffness and CT tumor enhancement ratio was calculated for tumors with or without MVI. The diagnostic performance [sensitivity, specificity, positive predictive value, negative predictive value, area under the curve (AUC)] and independent predicting factors for MVI were investigated.

Results: Finally, A total of 80 patients (aged 46.7±13.2 years) were enrolled, including 22 cases of tumors with MVI. The mean MRE stiffness of kidney parenchyma and kidney tumors was 4.8±0.2 and 4.5±0.7 kPa, respectively. There was significant difference in the mean MRE stiffness between tumors with MVI (5.4±0.6 kPa) and tumors without MVI (4.1±0.3 kPa) ($P<0.05$). The sensitivity, specificity, positive predictive value, negative predictive value, and the AUC for mean stiffness in the prediction of MVI were 100%, 75%, 63%, 96%, and 0.87 [95% confidence interval (CI): 0.72, 0.94], respectively. The corresponding values for the CT tumor enhancement ratio were 90%, 80%, 63%, 96%, and 0.88 (95% CI: 0.71, 0.93), respectively. The odds ratio (OR) value for MRE tumor stiffness and CT kidney tumor enhancement ratio in the prediction of MVI was 2.9 (95% CI: 1.8, 3.7) and 1.2 (95% CI: 1.0, 1.7), respectively ($P>0.05$).

Conclusions: 3D MRE imaging has promising diagnostic performance for predicting MVI in T1 stage ccRCC, which may improve the reliability of surgical strategy selection with T1 stage ccRCC.

Keywords: Kidney neoplasm; renal clear cell carcinoma; magnetic resonance elastography (MRE); microvascular invasion (MVI)

Submitted Feb 05, 2023. Accepted for publication Mar 20, 2023. Published online Mar 28, 2023.
doi: 10.21037/tau-23-94
View this article at: https://dx.doi.org/10.21037/tau-23-94

Introduction

Renal cell carcinoma (RCC) is the most common type of solid kidney tumor and accounts for 90% of all malignant kidney tumors. For T1N0M0 staging RCC, surgery is the best therapeutic strategy (1). This surgical strategy predominantly involves radical nephrectomy (RN) and partial nephrectomy (PN). For T1a staging (less than 4 cm in diameter) tumors, partial resection is preferred considering both the oncological perspective and the patient's quality of life. The Kidney Cancer Management Guide does not provide any high-quality evidence to support the selection of RN or PN for RCC with a T1b staging tumor (greater than 4 cm and less than 7 cm in diameter), although current guidelines do recommend RN for patients with venous tumor thrombi (1). It has been suggested that T1b and higher staging RCC is more likely to be accompanied by renal vein thrombosis than T1a staging RCC (2). Sugino *et al.* previously suggested that tumor cells growth into efferent veins (i.e., venules) was the first step of invasion into large blood vessels, which then gradually spread to the large and medium veins (3). Venules belong to the microvasculature. These are blood vessels including a tiny group of large veins, tumor capsules tiny venous vessels, and tiny segments within the tumor fibers, which can only be observed by microscopy. This means that microvascular invasion (MVI) is the first step in the pathway to the development of venous tumor thrombi. In this situation, RN is the preferred treatment strategy. Furthermore, multiple researchers have shown that MVI is an important factor in the prognosis of RCC (4-6). The diagnosis of MVI mainly based on histopathological analysis. There were few imaging biomarker have been reported to predict RCC MVI pre-surgery. Some previous reports (4) have indicated that tumor size is a major factor, since the RCCs in this study were T1 stage, the benefit of only evaluation of tumor size may be limited. Therefore, if we can accurately predict MVI prior to surgery, then we have more confidence selecting the appropriate form of surgical strategy for patients with RCC, thus improving the clinical management of these patients.

Magnetic resonance elastography (MRE) has emerged as a particularly useful non-contrast magnetic resonance imaging (MRI)-based technique that relies on the direct visualization of propagating shear waves in tissues. MRE has already been applied and validated in the kidneys, with data showing that this technique is feasible and reproducible in young healthy adults and kidney allografts (7,8). Moreover, tissue stiffness is not only affected by fibrosis, it can also be influenced by the microenvironment of tumor cells (9). Tumors with MVI are more invasive, which can be reflected by multiple aspects of the underlying composition and architecture of tumors (10,11). Prezzi *et al.* (12) explored the feasibility MRE for characterizing indeterminate small renal tumors and found that oncocytoma showed the higher shear wave attenuation values than renal carcinomas, which might reflect a high density of capillaries with normal endothelium in oncocytoma resulting in efficient energy dispersion in the form of heat, comparing with the disorganized vasculature and leaky endothelium typical in renal carcinomas. Tumors with MVI may have special a microenvironment of tumor cells such as incomplete capillaries endothelium, which may be reflected by MRE. Advanced three-dimensional (3D) MRE techniques, which are capable of acquiring and analyzing the internal wavefield in 3D space, address the technical limitations of standard 2D MRE techniques that are widely used for assessing liver fibrosis and may provide access to novel biomarkers.

In this study, we evaluated the performance of 3D spin echo-based echo planar imaging (SE-EPI) MRE for predicting MVI in T1 stage clear cell renal carcinoma (ccRCC) by histopathological analysis. We present the

Highlight box

Key findings

- Three-dimensional (3D) magnetic resonance elastography (MRE) has promising diagnostic performance for predicting microvascular invasion in T1 stage clear cell renal carcinoma (ccRCC), with similar diagnostic efficiency to the computed tomography (CT) tumor enhancement ratio.

What is known and what is new?

- Detection of microvascular invasion (MVI) of kidney tumors is important for selecting the optimal therapeutic strategy. Currently, the prediction of MVI lacks an accurate imaging biomarker.
- Our study evaluated the performance of 3D spin echo-based echo planar imaging (SE-EPI) MRE for predicting MVI in T1 stage ccRCC by histopathological analysis.

What is the implication, and what should change now?

- MVI is the first step in the pathway to the development of venous tumor thrombi in renal cell carcinomas, for which radical nephrectomy or partial nephrectomy is recommended. 3D MRE exhibited promising diagnostic performance for predicting MVI in patients with T1 stage ccRCC preoperatively. The application of this technique may improve the reliability of surgical strategy decision making and improve the clinical management of T1 stage ccRCC.

following article in accordance with the STARD reporting checklist (available at https://tau.amegroups.com/article/view/10.21037/tau-23-94/rc).

Methods

Ethics

The study was conducted in accordance with the Declaration of Helsinki (as revised in 2013). This study was approved by the Sichuan University West China Hospital institutional review board, ID: 20204#(1525)g and written informed consent was obtained from all patients prior to imaging.

Patients

This is a prospective study in a single-center, which was performed between April 2020 and May 2021. A total of 83 consecutive patients were enrolled in this study. All cases satisfied the following inclusion criteria: (I) the presence of a suspected ccRCC lesion as indicated by ultrasound or abdominal computed tomography (CT) examination that was no greater than 7 cm in diameter; (II) aged between 18 and 70 years; and (III) had availability of good quality images. Patients were excluded if any of the following applied: (I) evidence of contraindications to MRI; (II) patients had received tumor biopsy preoperatively; and (III) the presence of renal lesions that were not ccRCCs, as confirmed by post-surgical histopathology. A total of 3 patients were excluded, included 2 cases where the ccRCCs were not confirmed by histopathology and 1 case who presented with contraindications to MRI. Finally, a total of 80 patients were enrolled in this analysis.

MRI

All patients underwent pre-surgical imaging using a clinical 3.0 T MRI system (GE MR 750w) with an eighteen-channel array torso coil. The MRE was acquired along the coronal/axial plane of the kidneys. For all patients, image acquisition consisted of coronal T2-weighted imaging, axial T2-weighted imaging, and axial T1-weighted imaging for morphological evaluation of the kidneys and measurement of the tumor size.

An active MRE driver (Resoundant, Inc., Rochester, Minnesota, USA), located outside the scanner room was used to activate two passive drivers (flexible discs) positioned over each kidney. A long polyvinyl chloride (PVC) plastic tube was used to connect the active driver and the passive drivers. The passive driver was activated by varying acoustic pressures that were conducted via the plastic tube from the active driver.

Patients were imaged in the supine position. Passive drivers were held in place over kidneys by one operator to ensure they remained in the appropriate position; another operator used an elastic band to fix the drivers into position. 3D SE-EPI-MRE sequences were used to acquire 3D shear wave data. The imaging parameters were as follows: field of view (FOV) 40×40 cm, acquisition matrix 96×96, repetition time (TR) 1,600 ms, time to echo (TE) 54.2 ms; desired motion encoding gradient (MEG) frequency 80 Hz; MEGs were applied sequentially along all three orthogonal directions; frequency of applied motion 90 Hz (13,14); slice thickness 3.6 mm. The number of slices was 21, ensuring that we covered the entire kidney mass. The MRE sequence was completed within 1:08 minutes to allow for normal breathing in between breath holds (*Table 1*).

Subsequently, phase and magnitude images were generated for review and processing was performed, including phase unwrapping and spatio-temporal filtering in 20 evenly-spaced 3D directions. The 'magnitude of the complex shear modulus' was calculated using a 3D direct inversion algorithm in the units of kPa. This parameter, often referred-to as "shear stiffness", is dependent on both the elastic and viscous properties of the tissue.

CT

All patients underwent pre-surgical CT imaging with a multi-layer spiral Siemens CT scanning device (Erlangen, Germany). Image acquisition consisted of non-enhancement phase, cortical-medullar phase (40–50 s after injection of contrast media), and nephrographic phase (100–120 s after injection of contrast media). The parameters were as follows: slice thickness, 3 mm; tube voltage, 120 KV; tube current, 180 mA; reconstruction slice thickness, 0.75 mm; and slice spacing, 0.5 mm.

Imaging analysis

The 3D MRE sequences were automatically processed in the scanner and stiffness maps were generated and transferred to a post-processing workstation. The quality of MRE magnitude and wave images was evaluated initially by the reviewer, particularly with regards to whether the

Table 1 The imaging parameters for MRE-MRI, T1WI, and T2WI sequences

Parameter	MRE imaging	Coronal T2WI	Axial T2WI	Axial T1WI
Repetition time (ms)	1,600	1,000	1,650	150
Echo time (ms)	54.2	68	26	1.4/2
Flip angle (degrees)	180	150	111	75
Section thickness (mm)	3.6	3	5	5
Matrix#	96×96	320×256	320×256	256×205
Field of view* (mm)	400×400	452×452	378×276	438×285
Acquisition time (s)	1 min 8 s	27 s	1 min 7 s	33 s
MEG (Hz)	80	–	–	–
Direction of scan	Coronal/axial	Coronal	Axial	Axial
Breath-holding	Yes	Yes	Yes	Yes

Matrix# indicates the number of pixel in frequency coding direction × the number of pixel in phase coding direction. Field of view* indicates the image actual size in frequency coding direction × the image actual size in phase coding direction. MRE, magnetic resonance elastography; MRI, magnetic resonance imaging; T1WI, T1 weighted imaging; T2WI, T2 weighted imaging; MEG, motion encoding gradient.

contours of the kidney parenchyma and the contours of the kidney tumor could be clearly identified. Then, the stiffness value of the kidney parenchyma and the whole tumor were measured on a stiffness map using region-of-interest (ROI) analysis. These analyses referred to all anatomical sequences, and were copied onto the stiffness map. At all times, the reviewer was unaware of the histopathological analysis. The enhancement ratio was calculated as follows: the highest CT value (Hounsfield unit) of the kidney tumor divided by the CT value of the kidney cortex in cortical-medullar phase. This was drawn manually by ROI analysis by a reviewer who was unaware of the MRI images and the histopathological analysis.

Reference standards

Histopathological results served as the reference standard. A pathologist with more than seven years of experience who was unaware of clinical information and image test results assessed all the sections and provide histopathological results. The diagnosis included tumor category and the presence or absence of MVI. MVI was defined as a cancer cell nest with >50 cells in the endothelial vascular lumen under microscopy, according to the 'Guideline of Standardized Pathological Diagnosis of Primary Liver Cancer (2015 edition)' (15).

Statistical analysis

All statistical analyses were performed using SPSS version 19.0 software (SPSS, Chicago, IL, USA). The calculated minimum sample size required to predict MVI by MRE was 21 (MVI groups), 39 (non-MVI groups) respectively, and 18 (MVI groups), 37 (non-MVI groups) by CT, respectively. The intra-class correlation coefficient (ICC) was used to assess the inter-observer reproducibility of MRE and CT enhancement ratio.

During MRI image analysis, the reviewer drew the ROI on the MRE stiffness map, the MRE stiffness value was used for quantitative analysis. Normal distribution of the data was tested. The mean, standard error of the mean, and 95% confidence interval (CI) of the stiffness value for the kidney parenchyma and the whole tumor were then calculated. Differences in tumor size, mean perfusion between the solid part of stiffness in the presence or absence of MVI were assessed using the Student's *t*-test. A P value <0.05 was indicative of a significant difference. The relationship between tumor size, MRE stiffness value, and MVI according to histopathological analysis was assessed using Pearson's contingency coefficient. The diagnostic performance of the MRE stiffness value for predicting tumor MVI was assessed using the following diagnostic test indexes: sensitivity, specificity, positive predictive value,

Table 2 Demographic and clinical characteristics of the study population

Characteristic	ccRCC with MVI	ccRCC without MVI
Mean age[#] (y)	44.3±11.2	47.8±13.8
Gender		
Male	12	33
Female	10	25
Lesion location		
Left	14	30
Right	8	28
Tumor size*, cm	4.3±2.6	3.6±2.1
ISUP/WHO grade group		
Grade group 1	2	5
Grade group 2	4	13
Grade group 3	10	25
Grade group 4	6	15
Tissue acquisition method		
Radical nephrectomy	22	58
Partial nephrectomy	0	0

Mean age[#] and tumor size* are described as average value ± standard deviation. ccRCC, clear cell renal carcinoma; MVI, microvascular invasion; ISUP, International Society of Urologic Pathology; WHO, World Health Organization.

negative predictive value, and area under the curve (AUC).

In CT image analysis, the reviewer drew the ROI on CT images to measure kidney tumor enhancement ratio, the kidney tumor enhancement ratio was used for quantitative analysis. The mean, standard error of the mean, and 95% CI of the kidney tumor enhancement ratio was calculated. Differences in mean enhancement ratio between tumors with and without MVI were assessed using the Student's *t*-test. A P value <0.05 was indicative of a significant difference. The relationship between tumor enhancement ratio and MVI by histopathological analysis was evaluated using Pearson's contingency coefficient. The diagnostic performance of tumor enhancement ratio for predicting MVI in tumors was then investigated. DeLong test was used to compare overall accuracies (AUCs) of the MRE and contrast enhanced CT (CE-CT) methods. Logistic regression analysis was used to define the independent factors for predicting MVI.

Results

In total, 80 patients with 80 ccRCCs were enrolled in this study. The study cohort included 45 males and 35 females, with a mean age of 46.7±13.2 years. All patients received RN and were diagnosed histopathologically. The mean interval between MRI and histological analysis was 3.0±1.3 days. Histopathological analysis confirmed the presence of renal MVI in 22 patients, with 2 cases classified as T1a stage (*Table 2*). The mean tumor size with and without renal MVI was 4.3±2.6 and 3.6±2.1 cm, respectively. There was no significant difference between tumors with or without MVI (P>0.05).

MRE stiffness map

For inter-observer reproducibility, the ICC was 0.75 (95% CI: 0.7 to 0.82) for MRE, thus indicating good inter-observer reproducibility. The contours of the kidney were clearly identified in the MRE stiffness color map (*Figure 1*). The outer area of the kidney was masked and the kidney parenchyma showed high levels of stiffness. Kidney tumors with MVI also showed high levels of stiffness (*Figure 2*). Kidney tumors without MVI showed relatively lower levels of stiffness (*Figure 3*). The MRE stiffness shows normal distribution. The mean MRE stiffness for the kidney parenchyma and kidney tumors was 4.8±0.2 and 4.5±0.7 kPa, respectively. When considering tumors, the mean MRE stiffness of tumors with and without renal MVI was 5.4±0.6 and 4.1±0.3 kPa, respectively (*Figure 4*). The mean MRE stiffness differed significantly when compared between tumors with or without renal MVI (P<0.05).

CT images

For inter-observer reproducibility, the ICC was 0.82 (95% CI: 0.73 to 0.89) for CT images, indicating good inter-observer reproducibility. The highest enhancement area of the tumor could be clearly identified in CT images (*Figure 5*). The mean kidney tumor enhancement ratio in the cortical-medullar phase was 2.6. Within tumors, the mean kidney tumor enhancement ratio with and without renal MVI was 3.1±0.6 and 1.7±0.3, respectively. The mean tumor enhancement ratio differed significantly when compared between tumors with or without renal MVI (P<0.05).

Diagnostic performance

The Pearson's contingency coefficient when comparing

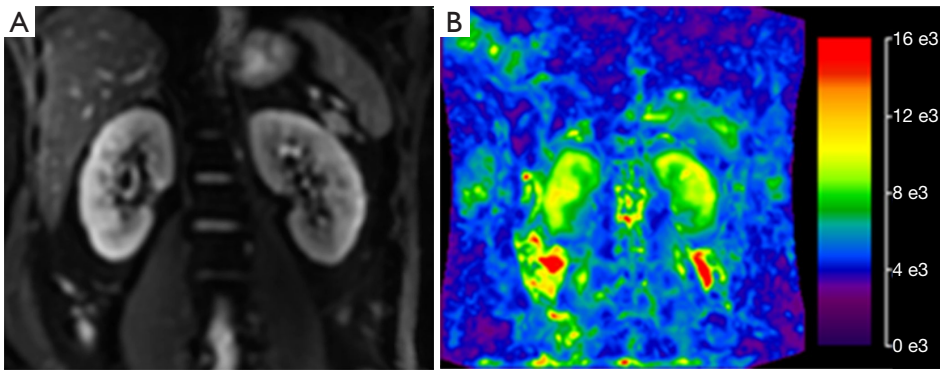

Figure 1 An MRE image of a normal kidney. (A) The magnitude map and (B) MIP of stiffness map. MRE, magnetic resonance elastography; MIP, maximum intensity projection.

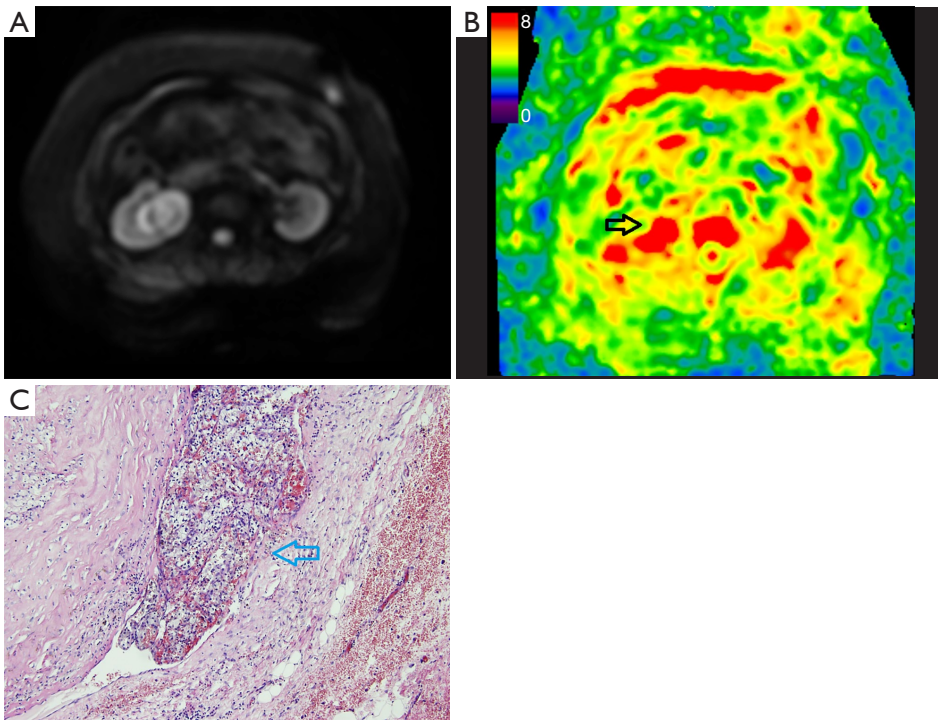

Figure 2 Magnetic resonance elastography images of a 50-year-old male with a right kidney tumor. (A) A magnitude map; (B) a stiffness map showing a red colored mass (black arrow) located in the right kidney, indicating the high stiffness of the tumor; and (C) a pathological hematoxylin-eosin staining section showing a cancer embolus (blue arrow) in the microvascular cavity. Original magnification ×100.

MVI with tumor size and MRE stiffness was 0.59 and 0.63, respectively. The sensitivity, specificity, positive predictive value, and negative predictive value for MRE stiffness in predicting MVI in tumors were 100%, 75%, 63%, and 96%, respectively. The AUC was 0.87 (95% CI: 0.72, 0.94) with a cut-off value of 5.0 kPa.

The Pearson's contingency coefficient between CT kidney tumor enhancement ratio and MVI was 0.61. The sensitivity, specificity, positive predictive value, and negative predictive value for the CT kidney tumor enhancement ratio in predicting MVI in tumors were 90%, 80%, 63%, and 96%, respectively. The AUC was 0.88 (95% CI: 0.71, 0.93) with a cut-off value of 2.6. DeLong test showed no significant difference between the AUCs of MRE and CE-CT.

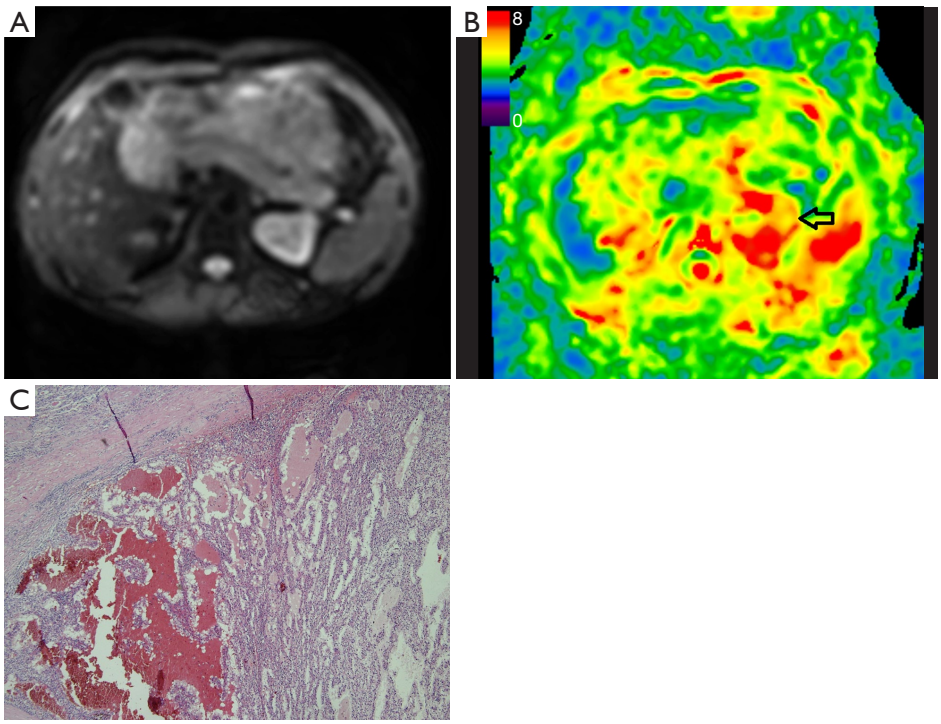

Figure 3 Magnetic resonance elastography images of a 63-year-old woman with a left kidney tumor. (A) A magnitude map; (B) a stiffness map showing a yellow colored mass (black arrow) located in the right kidney, indicating the low stiffness of the tumor; and (C) a pathological hematoxylin-eosin staining section showing no microvascular invasion. Original magnification ×100.

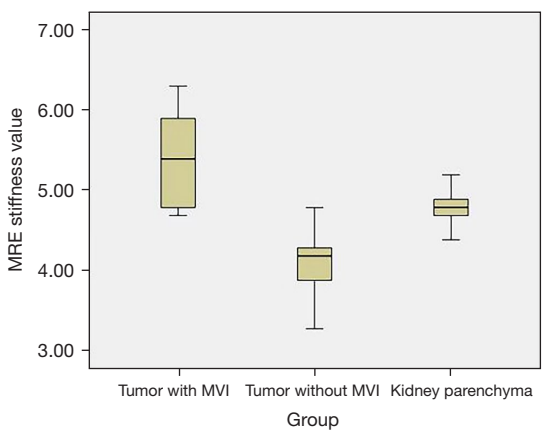

Figure 4 The mean, standard error of the mean, and 95% CI of the stiffness value for the kidney parenchyma and tumors with or without MVI. MRE, magnetic resonance elastography; MVI, microvascular invasion; CI, confidence interval.

Figure 5 The CT kidney tumor enhancement ratio calculations for patients. The ROIs were drawn in the highest enhancement area within the tumor and kidney parenchyma. CT, computed tomography; ROIs, regions of interests.

According to previous studies (4-6), age, hematuria, tumor size, MRE tumor stiffness, and CT kidney tumor enhancement ratio were included in the logistic regression analysis. The odds ratio (OR) value of MRE tumor stiffness and CT kidney tumor enhancement ratio to predict MVI in tumors was 2.9 (95% CI: 1.8, 3.7) and 1.2 (95% CI: 1.0, 1.7), respectively (P>0.05), while other factors had smaller OR values.

Discussion

This investigation was a prospective study analyzing the

used of 3D MRE to predict MVI in ccRCC. Our analyses demonstrated that 3D MRE exhibited promising diagnostic performance. The Kidney Cancer Management Guide does not currently provide any high-quality evidence to support which procedure (RN or PN) should be chosen for cases of RCC with a tumor diameter greater than 4 cm and less than 7 cm. Consequently, being able to determine the MVI of kidney tumors is important when selecting the optimal therapeutic strategy, since it is the first step in the formation of venous tumor thrombi. In the present study, only 9% of lesions with MVI were classified as T1a stage. This is consistent with the opinion that smaller lesions are less likely to undergo MVI. Interestingly, some previous reports (4) have indicated that tumor size is a major factor related to MVI. However, in the current study the mean tumor size with and without renal MVI showed no significant difference, possibly because tumors in this study were mainly T1 stage which may have limited the analysis of the effect of tumor size on MVI. Authors inferred that the tumor size may not be a major factor in early stage of tumor.

In this investigation, we showed that the sensitivity, specificity, and negative predictive value were relatively high, thus indicating that MRE stiffness is a promising parameter with which to predict tumor MVI. The ROI on the stiffness map was placed to cover the whole tumor since the lower spatial resolution made it difficult to define the exactly solid part of the tumor. Meanwhile, the ROI on the CT was placed only on the area showing the highest CT value, due to the high spatial resolution. In our study, tumors with MVI had a higher stiffness; this may be due to the fact that tumors with MVI are more invasive, have higher cellular density, more extracellular collagen, and higher blood flow, thus influencing tissue stiffness (12). The positive predictive value was relatively low, suggesting a part of the tumor without MVI had high levels of stiffness; this may reflect the fact that complex factors influence the stiffness of tissues. Other functional MRI techniques like intravoxel incoherent motion DWI imaging (16), arterial spin labelling (17) could be combined with MRE to increase the positive predictive value. We found that tumors without MVI were softer (with a lower stiffness) than the renal parenchyma, this may be due the heterogeneity of ccRCCs. The whole blood flow (including the cystic/necrotic part) may be lower than the renal parenchyma. Furthermore, tumors without MVI are usually a lower pathological stage (18,19). Consequently, cellular density may not be sufficient to create a high level of stiffness. Previous investigations have used multiple forms of MRI to predict MVI in tumors, however, these studies were mainly focused on the liver (20-22). Our present report provides addition new knowledge relating to the clinical application of this technique for renal cancer.

In the logistic regression analysis, the OR value of MRE tumor stiffness was higher than the CT kidney tumor enhancement ratio in predicting MVI, however, there was no significant difference. Although the two factors showed a significant difference in the univariable analysis, the multivariable analysis indicated they were not independent predictive factors for MVI. Therefore, using a simple imaging factor may be insufficient and future large sample research involving a combination of clinical factors may be useful. However, since the major imaging factor predicting MVI showed no significant difference in T1 staging tumors, MRE tumor stiffness may still be seen as useful information to predict MVI.

Previous studies have used MRE to characterize small renal tumors and reflect the underlying tumor composition (cellular density, extracellular collagen, the accumulation of hydrophobic and disorganized proteins, hemorrhage, and necrosis) and architecture (cellular and connective tissue distribution, vascular size, density, and permeability) (12,23,24). Tumors with MVI are usually more malignant, with some previous studies showing that malignancy increases stiffness via the deposition of collagen in the extracellular matrix and increased levels of interstitial pressure arising from alterations in the vasculature (12). This forms the theoretical basis for using MRE to predict MVI. High grade clear cell carcinoma may be associated with increased cellular density and an increased amount of fibrous stroma; these factors would be expected to increase the stiffness of tumors.

Over recent years, an increasing number of studies have explored the use of MRE, especially hepatic fibrosis, evaluation of liver regeneration following hepatectomy in hepatocellular carcinoma, skeletal muscle and kidney allograft (25-28). MRE can be used to quantify tissue stiffness by visualizing the propagation of shear waves in the tissue. In response, shear waves are generated and then propagated in the tissue; these waves can then be imaged using a phase contrast sequence. The speed of the wave propagation is dependent on organ stiffness. Stiffer tissue promotes waves that propagate faster and have longer wavelengths. By processing images of these waves it is possible to generate a tissue stiffness map (29). In view of the small size of the kidneys, a higher frequency (90 or 120 Hz)

needs to be used than with the liver and a 3D MRE technique similar to that used for MRE would be needed (29). The use of a 3D MRE sequence with improved resolution may be beneficial to address partial volume effects in small tumor lesions. In a previous study, Gandhi *et al.* performed kidney MRE on 33 healthy subjects and demonstrated the reproducibility and good agreement of SE-EPI (30).

3D MRE allows us to encode motion in all three dimensions and process non-planar waves with better lesion evaluation. This technique only requires a short examination time and does not involve ionizing radiation. Failure to obtain good contact between the patient and the passive driver can result in poor transmission of the waves. Enhancement CT can rapidly form an image and can be used to accurately measure the tumor enhancement ratio by CT value; however, a key disadvantage of this method is the need for ionizing radiation. For patients with renal insufficiency, the use of iodine contrast agent should be considered very carefully.

Multiple studies (31,32) have proposed that factors related to irregular tumor margin and enhancement (peritumoral or intratumoral regions) are important for the prediction of MVI. Since all patients with kidney tumors admitted to our hospital underwent enhancement abdomen CT prior to surgery as a regular examination, the enhancement ratio of kidney tumors was used for comparison with MRE instead of MRI enhancement. In the present study, we found that the diagnostic performance of predicting MVI using MRE was comparable to that of the kidney tumor enhancement ratio assessed by CT.

Previous studies demonstrated that some MRI features are associated with MVI. Dai *et al.* used radiomics features extracted from MRI to predict MVI in patients with hepatocellular carcinoma and found that a radiomics model based on images of the hepatobiliary phase showed better predictive performance than other phases (33). Tang *et al.* studied 273 patients with hepatocellular carcinoma and found that the key imaging predictors of MVI included tumor size, the capsule, and rim enhancement (34). Chen *et al.* used conventional enhanced MRI features to predict MVI in hepatocellular carcinoma and found that the apparent diffusion coefficient (ADC) value, non-smooth tumor margin, showed high levels of diagnostic accuracy (35). This may be a reminder that multiple sequences are advantageous when predicting MVI. Since MRE can reflect key information relating to a tumor by determining stiffness, this technique may be very promising in predicting MVI.

There were some limitations in this analysis. First, due to the limited availability of MRE, this was a single-center exploratory study. In the future, it will be necessary to perform multiple-center studies. Second, in our study, we considered the difference in stiffness between kidney tumors with and without MVI. However, our analyses lacked an explanation relating to the exact pathological process, which referred to the respective contribution of blood flow, fibrosis, collagen, cellular density, or other aspects of composition and architecture to stiffness. These factors should be analyzed in future research.

Conclusions

This study demonstrates that 3D MRE has promising diagnostic performance for predicting MVI in patients with T1 stage ccRCC preoperatively. The application of this technique may improve the reliability of surgical strategy selection and improve the clinical management of patients with T1 stage ccRCC.

Acknowledgments

The authors wish to thank Professor Richard Ehman and his team from the Mayo Clinic for technique support and manuscript editing.
Funding: This research was supported by National Natural Science Foundation of China (grant No. 81801671), the Sichuan Provincial Science and Technology plan Grans (grant No. 2019YFS0445), the US National Institutes of Health (grant No. R01 EB001981), the Imaging Biomarker program in the Center for Individualized Medicine (CIM) at Mayo Clinic, and the Hainan Province Clinical Medical Center.

Footnote

Reporting Checklist: The authors have completed the STARD reporting checklist. Available at https://tau.amegroups.com/article/view/10.21037/tau-23-94/rc

Data Sharing Statement: Available at https://tau.amegroups.com/article/view/10.21037/tau-23-94/dss

Peer Review File: Available at https://tau.amegroups.com/article/view/10.21037/tau-23-94/prf

Conflicts of Interest: All authors have completed the ICMJE uniform disclosure form (available at https://tau.amegroups.

com/article/view/10.21037/tau-23-94/coif). The authors have no conflicts of interest to declare.

Ethical Statement: The authors are accountable for all aspects of the work in ensuring that questions related to the accuracy or integrity of any part of the work are appropriately investigated and resolved. The study was conducted in accordance with the Declaration of Helsinki (as revised in 2013). This study was approved by the Sichuan University West China Hospital institutional review board, ID: 20204#(1525)g and written informed consent was obtained from all patients prior to imaging.

References

1. Ljungberg B, Bensalah K, Canfield S, et al. EAU guidelines on renal cell carcinoma: 2014 update. Eur Urol 2015;67:913-24.
2. Kirkali Z, Van Poppel H. A critical analysis of surgery for kidney cancer with vena cava invasion. Eur Urol 2007;52:658-62.
3. Sugino T, Yamaguchi T, Hoshi N, et al. Sinusoidal tumor angiogenesis is a key component in hepatocellular carcinoma metastasis. Clin Exp Metastasis 2008;25:835-41.
4. Kwon SY, Lee JN, Kim BS, et al. Impact of Microvascular Invasion and Tumor Necrosis on the Prognosis of Korean Patients with pT1b Renal Cell Carcinoma. Urol Int 2015;95:65-71.
5. Huang H, Pan XW, Huang Y, et al. Microvascular invasion as a prognostic indicator in renal cell carcinoma: a systematic review and meta-analysis. Int J Clin Exp Med 2015;8:10779-92.
6. Santiago-Agredano B, Álvarez-Kindelán J, Font-Ugalde P, et al. Prognostic value of microvascular invasion in predicting survival in renal cell carcinoma. Actas Urol Esp 2013;37:504-12.
7. Rouvière O, Souchon R, Pagnoux G, et al. Magnetic resonance elastography of the kidneys: feasibility and reproducibility in young healthy adults. J Magn Reson Imaging 2011;34:880-6.
8. Kim JK, Yuen DA, Leung G, et al. Role of Magnetic Resonance Elastography as a Noninvasive Measurement Tool of Fibrosis in a Renal Allograft: A Case Report. Transplant Proc 2017;49:1555-9.
9. Warner L, Yin M, Glaser KJ, et al. Noninvasive In vivo assessment of renal tissue elasticity during graded renal ischemia using MR elastography. Invest Radiol 2011;46:509-14.
10. Shi X, Young CD, Zhou H, et al. Transforming Growth Factor-β Signaling in Fibrotic Diseases and Cancer-Associated Fibroblasts. Biomolecules 2020;10:1666.
11. Vlodavsky I, Gross-Cohen M, Weissmann M, et al. Opposing Functions of Heparanase-1 and Heparanase-2 in Cancer Progression. Trends Biochem Sci 2018;43:18-31.
12. Prezzi D, Neji R, Kelly-Morland C, et al. Characterization of Small Renal Tumors With Magnetic Resonance Elastography: A Feasibility Study. Invest Radiol 2018;53:344-51.
13. Hoodeshenas S, Yin M, Venkatesh SK. Magnetic Resonance Elastography of Liver: Current Update. Top Magn Reson Imaging 2018;27:319-33.
14. Kennedy P, Bane O, Hectors SJ, et al. Magnetic resonance elastography vs. point shear wave ultrasound elastography for the assessment of renal allograft dysfunction. Eur J Radiol 2020;126:108949.
15. Cong WM, Bu H, Chen J, et al. Practice guidelines for the pathological diagnosis of primary liver cancer: 2015 update. World J Gastroenterol 2016;22:9279-87.
16. Kalage D, Gupta P, Gulati A, et al. Multiparametric MR imaging with diffusion-weighted, intravoxel incoherent motion, diffusion tensor, and dynamic contrast-enhanced perfusion sequences to assess gallbladder wall thickening: a prospective study based on surgical histopathology. Eur Radiol 2023. [Epub ahead of print]. doi: 10.1007/s00330-023-09455-w.
17. Zhang HM, Wen DG, Wang Y, et al. Arterial Spin Labeling MRI for Predicting Microvascular Invasion of T1 Staging Renal Clear Cell Carcinoma Preoperatively. Front Oncol 2021;11:644975.
18. Delahunt B, Eble JN, Samaratunga H, et al. Staging of renal cell carcinoma: current progress and potential advances. Pathology 2021;53:120-8.
19. Isik B, Gonultas F, Sahin T, et al. Microvascular Venous Invasion in Hepatocellular Carcinoma: Why Do Recurrences Occur? J Gastrointest Cancer 2020;51:1133-6.

20. Hong SB, Choi SH, Kim SY, et al. MRI Features for Predicting Microvascular Invasion of Hepatocellular Carcinoma: A Systematic Review and Meta-Analysis. Liver Cancer 2021;10:94-106.
21. Zhou W, Jian W, Cen X, et al. Prediction of Microvascular Invasion of Hepatocellular Carcinoma Based on Contrast-Enhanced MR and 3D Convolutional Neural Networks. Front Oncol 2021;11:588010.
22. Song D, Wang Y, Wang W, et al. Using deep learning to predict microvascular invasion in hepatocellular carcinoma based on dynamic contrast-enhanced MRI combined with clinical parameters. J Cancer Res Clin Oncol 2021;147:3757-67.
23. Fujii Y, Sato Y, Suzuki H, et al. Molecular classification and diagnostics of upper urinary tract urothelial carcinoma. Cancer Cell 2021;39:793-809.e8.
24. Hectors SJ, Lewis S. Tomoelastography of the Prostate: Use of Tissue Stiffness for Improved Cancer Detection. Radiology 2021;299:371-3.
25. Han JH, Ahn JH, Kim JS. Magnetic resonance elastography for evaluation of renal parenchyma in chronic kidney disease: a pilot study. Radiol Med 2020;125:1209-15.
26. Yu YM, Ni QQ, Wang ZJ, et al. Multiparametric Functional Magnetic Resonance Imaging for Evaluating Renal Allograft Injury. Korean J Radiol 2019;20:894-908.
27. Li Y, Gao Q, Chen N, et al. Clinical studies of magnetic resonance elastography from 1995 to 2021: Scientometric and visualization analysis based on CiteSpace. Quant Imaging Med Surg 2022;12:5080-100.
28. Zhang T, Li Q, Wei Y, et al. Preoperative evaluation of liver regeneration following hepatectomy in hepatocellular carcinoma using magnetic resonance elastography. Quant Imaging Med Surg 2022;12:5433-51.
29. Jiang K, Ferguson CM, Lerman LO. Noninvasive assessment of renal fibrosis by magnetic resonance imaging and ultrasound techniques. Transl Res 2019;209:105-20.
30. Gandhi D, Kalra P, Raterman B, et al. Magnetic Resonance Elastography of kidneys: SE-EPI MRE reproducibility and its comparison to GRE MRE. NMR Biomed 2019;32:e4141.
31. Kim TM, Lee JM, Yoon JH, et al. Prediction of microvascular invasion of hepatocellular carcinoma: value of volumetric iodine quantification using preoperative dual-energy computed tomography. Cancer Imaging 2020;20:60.
32. Ünal E, İdilman İS, Akata D, et al. Microvascular invasion in hepatocellular carcinoma. Diagn Interv Radiol 2016;22:125-32.
33. Dai H, Lu M, Huang B, et al. Considerable effects of imaging sequences, feature extraction, feature selection, and classifiers on radiomics-based prediction of microvascular invasion in hepatocellular carcinoma using magnetic resonance imaging. Quant Imaging Med Surg 2021;11:1836-53.
34. Tang M, Zhou Q, Huang M, et al. Nomogram development and validation to predict hepatocellular carcinoma tumor behavior by preoperative gadoxetic acid-enhanced MRI. Eur Radiol 2021;31:8615-27.
35. Chen Y, Xia Y, Tolat PP, et al. Comparison of Conventional Gadoxetate Disodium-Enhanced MRI Features and Radiomics Signatures With Machine Learning for Diagnosing Microvascular Invasion. AJR Am J Roentgenol 2021;216:1510-20.

(English Language Editor: J. Teoh)

Cite this article as: Zhang HM, Wen DG, Chen J, Chen YT, Yin M, Wang Y, Wei Y, Bao YG, Wu YH, Song B. A diagnostic test of three-dimensional magnetic resonance elastography imaging for preoperative prediction of microvascular invasion in patients with T1 stage clear cell renal carcinoma. Transl Androl Urol 2023;12(3):466-476. doi: 10.21037/tau-23-94

